JOURNAL OF SOLID STATE CHEMISTRY 9, 368–374 (1974)

New Phases with Fluorite-Derived Structure in CaF_2–(Y, Ln)F_3 Systems*

P. P. FEDOROV, O. E. IZOTOVA, V. B. ALEXANDROV, AND B. P. SOBOLEV

Institute of Crystallography, Academy of Sciences, Moscow, U.S.S.R.

Received May 30, 1973

Crystallographic characteristics of six new phases of idealized composition $Ca_8R_5F_{31}$ which are formed in the CaF_2–RF_3 (R = Y, Ho-Lu) systems are reported. All the phases have a similar structure derived from CaF_2 with slight distortion and pseudocubic unit cell parameters $a_{\mathrm{ord}} = 13a_{\mathrm{dis}}$ (where a_{dis} is the parameter of the fluorite subcell). The degree of ordering increases in the lanthanide series with decrease of ionic radius and, in every system given, with an increase in the RF_3 content of the solid solution. Significant influence of temperature and time of annealing on the degree of ordering was not detected.

Introduction

In all the CaF_2–RF_3 systems (R = yttrium, lanthanum, and rare earth elements), phases of variable composition with fluorite structure have been detected [see review (*1*)]. Goldschmidt (*2*) in 1923 suggested for these solid solutions a substitution model $Ca^{2+} \rightarrow R^{3+} + F^-$ which was confirmed by density measurements, and which has served since then as an example in crystallochemistry courses of isomorphism with filling in of space. Recent precise measurements of density (*3*) have shown small deviations from those calculated according to the model of (*2*).

N. V. Belov again pointed out in 1956 (*4*) the crystallochemical inadequacy of Goldschmidt's substitution model, according to which "extra" fluorine atoms are placed in the centers of large cubic (for fluorine) cavities of the fluorite structure $\{xxx\}$ with $x = 0.5$, where they appear in an unusual anionic environment and are supposed to reduce their radii by ~30%.

X-ray study of the detailed atomic structure of $Ca_{0.607}Ce_{0.393}F_{2.393}$ (*5*) showed its essential difference from the proposition of (*2*) and, from the experimental data, led to a new scheme of isomorphous substitution $Ca^{2+} + F_I^- \rightarrow Ce^{3+} + 2F_{II}^-$, where fluorine atoms in the original structure (corners of the coordination cubes) are marked by the symbol I and fluorine atoms in new positions, $\{xxx\}$ with $x = 0.421$, by the symbol II. The existence of interstitial ions of type F_{II}^- has also been shown by neutron diffraction study of the solid solution $Ca_{0.9}Y_{0.1}F_{2.1}$ (*6*). In the given domain of RF_3 concentration in the CaF_2–RF_3 systems, the scheme of isomorphous substitution of Ca^{2+} for R^{3+} found in (*5*) is apparently realized for the whole range of systems of rare earth trifluorides from "large" La^{3+} and Ce^{3+} to "small" Lu^{3+}, since Y^{3+} in crystallochemical behavior models that of the trifluorides of the "heavy" lanthanides. The statistical pattern of the distribution of interstitial fluorine atoms and of anion vacancies in the structures of the $Ca_{1-x}R_xF_{2+x}$ solid solutions leads to preservation of the symmetry and order of magnitude of the fluorite unit cell, although the symmetry of individual fragments of the structure undergoes basic changes. The special features of the crystal structure of these phases appear graphically in the optical spectra of the rare earth ions in crystals of two-component (and more complex) compositions (*7*), which indicates formation, starting with a small content of RF_3, of a large number of kinds of coordination polyhedra not predicted by the model in (*2*).

The similarity of crystallochemical properties of Ca^{2+} and (Y, Ln)$^{3+}$ explains, as a rule, the mutual substitutability of these ions over broad ranges without ordering. However, in our case one might expect that a high concentration of defects in the anionic motif [i.e., the high solubility of RF_3 in CaF_2 (*8*)], which in a certain sense is unique for ionic crystals, leads under certain

---

* Original manuscript received in Russian. Copy available on written request to the Editors.

Printed in Great Britain

conditions to formation of phases with ordered distribution of such defects.

The possibility of formation in principle of ordered phases during heterovalent substitution of M^{2+} for R^{3+} in a fluorite structure type was shown in the instance of SmF_2–SmF_3 and EuF_2–EuF_3 systems (*9*, *10*) and also in MF_2–RF_3 systems ($M = Ca$, Sr, Pb; $R^{3+} = Tl$, Ti, V, Cr, Fe, Ga) (*11–17*). The composition of such phases varies within wide limits all the way to 40 mole% RF_3 (rhombic distortion type prevails). We found different types of ordered phases in BaF_2–(Y, Ln)F_3 (*18*) and SrF_2–LnF_3 (*19*) systems, some of which were isolated in the form of single crystals.

In CaF_2–(Y, Ln)F_3 systems, despite many reports in the literature including even the recent (*20*), through X-ray analysis of the variable composition phases $Ca_{1-x}(Y, Ln)_xF_{2+x}$, up to now not even in one has there been noted alteration of the fluorite structure of solid solutions based on CaF_2. In detailing these sections of the phase diagrams (composition intervals from 0.2 to 3 mole% and temperature ~50°C), we discovered in systems with trifluorides of yttrium and the "heavy" lanthanides from holmium to lutetium, inclusive, phases of structure derived from fluorite. The present work is devoted to a description of these well-ordered phases.

Experimental Procedure

Samples of $Ca_{1-x}R_xF_{2+x}$ solid solutions were obtained by reaction in the solid phase of CaF_2 with the corresponding RF_3 without superheating above the temperature where equilibrium is established. Annealing was carried out in nickel containers in a fluorinating atmosphere; the oxygen content in the specimens after thermal treatment, as determined by vacuum fusion, did not exceed 0.20% by weight. Variation in the oxygen content from 0.02 to 0.20% by weight had no noticeable effect on the phase composition. Phase equilibria were investigated in the temperature range 870–1070°C; length of annealing varied from 220 to 110 hr. The containers with the samples were quenched in running water.

In addition to the method described, we also reproduced previously used methods for getting $Ca_{1-x}R_xF_{2+x}$ solid solutions by cooling of melts, varying also the fluorinating atmosphere (HF). In all cases we obtained the ordered phases described below. Consequently, the lack of information in the literature on ordering in $Ca_{1-x}R_xF_{2+x}$ evidently can be explained by insufficient carefulness in studying the CaF_2–RF_3 systems.

Phase composition was determined with X-rays on a AFV-201 (Japan) diffractometer; the radiation was $CuK\alpha$. Parameters of the unit subcells of the $Ca_{1-x}R_xF_{2-x}$ solid solutions were calculated from the (400) reflection, CaF_2, $a = 5.46295 \pm 0.00010$ Å (*21*), serving as internal standard. The accuracy for determining the fluorite subcells works out to be ±0.003 Å.

Single crystals were studied by Laue and oscillation methods and by photographing the reciprocal lattice. $FeK\alpha$ radiation was used for best resolution of reflections from phases with large unit cell dimensions. Unit cell parameters in a series of cases were defined more precisely on a single crystal diffractometer using pinacoid reflections of high order ($2\theta > 120°$).

Results of the Experiments and Discussion

Powder X-rays of $Ca_{1-x}R_xF_{2+x}$ solid solutions, where $x = 0.35$–0.40 ($R = Y$, Ho–Lu), revealed images that were superlatticed in relation to the CaF_2 type. A typical X-ray of the powder of an ordered phase is presented in Fig. 1a. In the CaF_2–HoF_3 and CaF_2–YF_3 systems at an RF_3 content of 37–40 mole%, only very diffuse maxima were noted on the diffraction patterns instead of superlattice images. In solid solutions with identical content of the various RF_3, the sharpness of the superstructure grew noticeably in passing from Ho^{3+} to Lu^{3+}. The same thing was noted for each rare earth element when its content in the solid solution was increased (Fig. 1a–e). The definition of the superlattice images which was clearly determined by the two factors enumerated above (the ionic radius of R^{3+} and the RF_3 content in the solid solution), did not, in fact, depend on the duration and temperature of annealing. Apparently, the definition of these images characterizes the degree of ordering of the solid solutions [see (*22*), for example].

Thus, in our case, the degree of ordering of $Ca_{1-x}R_xF_{2+x}$ solid solutions depends on the composition of the phase. For rare earth elements with ionic radius larger than that of Ho^{3+}, the appearance of ordering at the extreme outer limits of composition was not observed in a distinct form (on the X-rays of the powder) in the temperature range we studied. The character of the ordering (cf. Fig. 1a) was identical for the whole series of systems listed above.

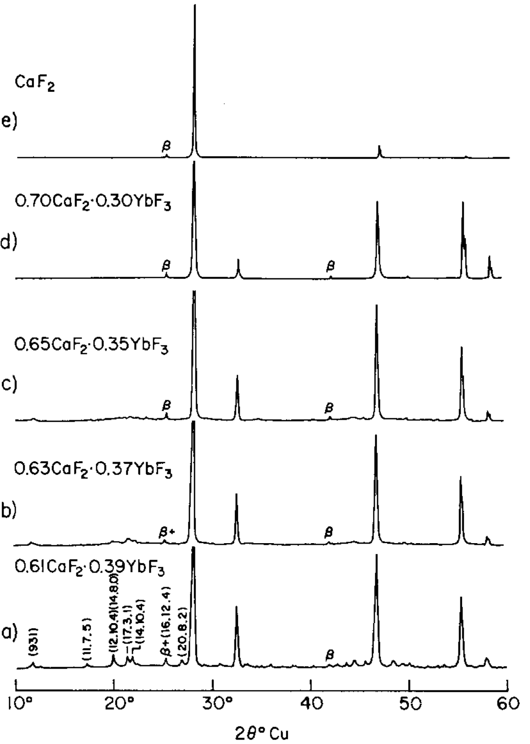

FIG. 1 (a–e). Powder X-ray diagrams of solid solutions $Ca_{1-x}Yb_xF_{2+x}$ ($0 \leq x \leq 0.39$) at 1067°C isotherm.

Single crystals appropriate for X-ray study were selected from samples with gross composition from $Ca_{0.6}R_{0.4}F_{2.4}$ to $Ca_{0.5}R_{0.5}F_{2.5}$. The cubic symmetry of ordered phase specimens was established by the Laue method. Analysis of the distribution and relative intensity of spots on the Laue pictures confirmed the presence of triple and quadruple axes of symmetry. For a saturated solid solution of TmF_3 in fluorite, the unit cell parameter was determined as $a = 71.80 \pm 0.15$ Å by oscillation around [100] and [110]. This magnitude corresponds to a 13-fold increase in the parameter of the original unordered fluorite subcell (a_{dis}). In rotation photographs (Fig. 2), the period $a_{\text{dis}} = a_{\text{ord}}/13$ was expressed very sharply: reflections of the 0 and 13th layer lines were 50–100 times more intense than the rest. Defining the parameters more precisely on powder led to the same value of $a_{\text{ord}} = 71.77 \pm 0.04$ Å.

The relation of the identity periods along [100], [110], and [111] showed that the cell was face-centered. On powder X-rays of the ordered phases, we noted weak splitting of the basic (fluorite) reflections. The type of splitting of the powder X-ray and rotation images (Fig. 2) indicates the rhombohedral nature of the distortion of the fluorite subcell. The degree of deformation is very small—the rhombohedral angle of the phase $Ca_{0.6}Tm_{0.4}F_{2.4}$ amounts to 60°08′.

Rhombohedral distortion of the cubic cell should lead to splitting of the reflections of type (*hhh*) in the powder X-rays, whereas individual reflections from single crystals would remain single. In our case, splitting of (*hhh*) was observed in X-rays of the powder and in rotation photographs as well as in the case of a survey of individual reflections on the single crystal diffractometer. Evidently, we are dealing not with a single crystal but with submicroscopic intergrowths of rhombohedral domains, the three-fold axes of

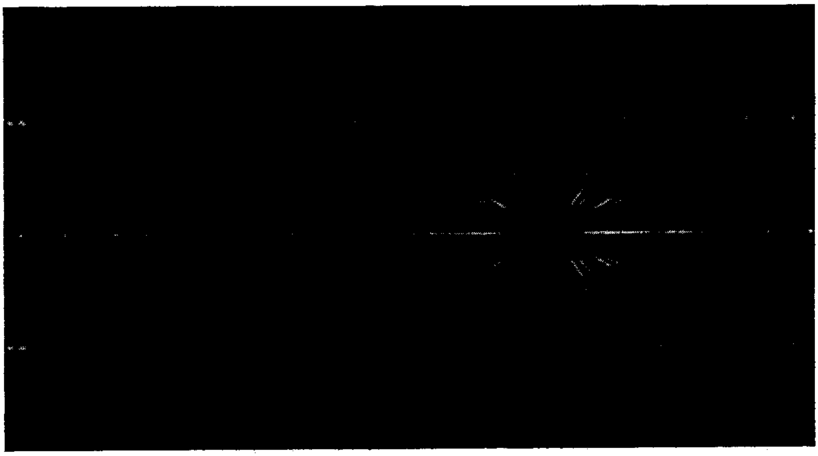

FIG. 2. Rotation X-ray photograph along second-order axis of a single crystal $Ca_{0.6}Tm_{0.4}F_{2.4}$ with unfiltered Cu radiation.

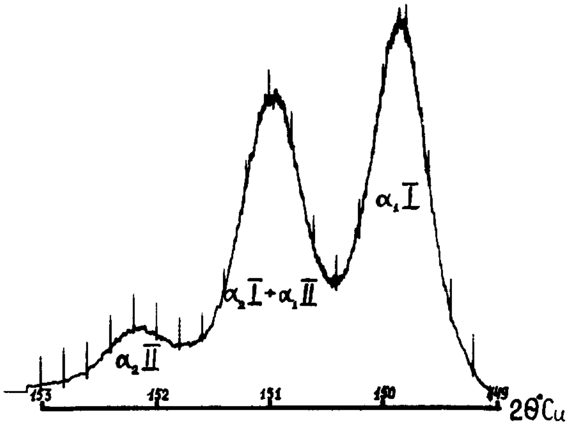

FIG. 3. Splitting of the fluorite reflection (444) in a single crystal of ordered phase $Ca_{0.6}Tm_{0.4}F_{2.4}$ (diffractometer exposure, $CuK\alpha_1,\alpha_2$).

which are statistically oriented along all four of the "three-fold" axes of the cubic pseudocell. This circumstance does not permit us to determine unambiguously whether the 13-fold increase in the identity period mentioned above is related to the cell as a whole or to one of its axes (*a* or *c* in the hexagonal aspect). The statistical character of the orientation of domains is confirmed by the intensity ratio of the components of the split "fluorite" reflection (444) in the diffraction pattern of a single crystal (Fig. 3). In ideally statistical distribution, the ratio should be 6:5:1. Anisotropic regions in grains of ordered phase were not observed in transparent thin sections, which also speaks of the extremely small dimensions of the domains.

TABLE I

POWDER X-RAY DATA OF $Ca_{0.6}Tm_{0.4}F_{2.4}$[a]

No.	d (Å)	(h k l)	I/I_0	No.	d (Å)	(h k l)	I/I_0
1.	7.52	(9. 3. 1)	4	17.	2.240	—	2
2.	7.06	(8. 6. 2)	0.5	18.	2.119	—	2
3.	5.131	(11. 7. 5)	2	19.	2.075	—	3
4.	4.440	(12.10. 4) (14. 8. 0)	12	20.	2.042	—	5
5.	4.147	(17. 3. 1)	7	21.	1.9917	—	5
6.	4.058	(14.10. 4)	7	22.	1.9880	—	4
7.	3.524	β^+(16.12. 4)	3	23.	1.9524[b]	—	60
8.	3.315	(20. 8. 2)	3	24.	1.8851	—	4
9.	3.186	(13.13.13)	100	25.	1.8814	—	4
10.	2.904	—	3	26.	1.8491	—	4
11.	2.760	(26. 0. 0)	36	27.	1.8451	—	3
12.	2.685	—	3	28.	1.8267	—	2
13.	2.661	—	2	29.	1.7146	—	2
14.	2.505	—	2	30.	1.6658[b]	—	34
15.	2.413	—	1	31.	1.5943	—	9
16.	2.360	—	1	32.	1.5912	—	7
				33.	1.3804	(52.0.0)	3

[a] Annealing: 1067°C, 110 hr.

[b] Lines split.

In view of the impossibility of determining the true parameters of the rhombohedral unit cell, further study of the ordered phases in the CaF_2–(Y, Ln)F_3 systems will be carried out in terms of a cubic pseudocell where $a_{ord} = 13a_{dis}$.

From the multiple of elementary pseudocells of ordered phases with fluorite subcells ($a_{ord} = 13a_{dis}$) and the number of formula units $Ca_{1-x}R_xF_{2+x}$ per fluorite subcell ($Z = 4$), one can calculate the possible compositions with maximum ordering assuming full occupancy of cation positions. The composition of such a phase is expressed by the general formula $Ca_mR_nF_{2m+n}$. A cell with the parameter $a_{ord} = 13a_{dis}$ contains $4 \times 13^3 = 8788$ cations. In order that the number of formula units $Z = 8788/(m + n)$ be whole, the sum $(m + n)$ must be equal to one of the ten divisors of the number 8788. The simplest homogeneous composition with (for a given RF_3) fully formed superstructure which is nearest the two-phase region is $Ca_8R_5F_{31}$ (38.5 mole% RF_3, $m + n = 13$). According to the data of X-ray and crystal-optic analyses for all the systems CaF_2–(Y, Ln)F_3 (Ln = Ho – Lu) where ordering was noted, the maximum content of RF_3 in the solid solutions is practically independent of the size of R^{3+} and amounts to 39 ± 0.5 mole%. On raising of the temperature from 90 to 1000°C, the solubility slightly increases (to 40 ± 0.5 mole%).

Table I gives a listing of the interplanar spacings for maximum ordered phases in the system CaF_2–TmF_3. Indexing of the powder X-rays over the whole range of angles is without meaning for large unit cell parameters; consequently, we carried out this operation only for the early reflections (correction was done through α-SiO_2). It turned out that only the 11- and 13-fold (the former was worse) increase of the original fluorite subcell parameters led to satisfactory indexing of the first seven reflections with indices allowed for the *F*-lattice (selection of possible values for the indices was made on the basis of rotation photographs).

The cubic pseudocell parameters of the ordered phases which were obtained from indexing the powder X-rays are presented in Table II. In all the systems they were determined for the saturated solid solutions with overall RF_3 content of 45 mole% (the compositions were two-phase; the temperature at which they were obtained was 1008°C.) The question of the exact composition of the ordered phases in the CaF_2–RF_3 systems needs further study. Because of the considerations mentioned above, an idealized composition of $Ca_8R_5F_{31}$ was adopted in this work.

The intensity of the superlattice reflections in the powder X-rays decreases with RF_3 content so that at 25–30 mole%, they are not experimentally detected (Fig. 1). Definition of the superlattice in $Ca_{1-x}R_xF_{2+x}$ increases gradually with increase in x; however, in a narrow range (2–3 mole%) of compositions near $x = 0.385$, the degree of ordering increases sharply.

The character of the ordering is well-illustrated by the Laue photographs of single crystals of $Ca_{1-x}R_xF_{2+x}$, presented in Fig. 4. Figure 4a was obtained on a single crystal of $Ca_{0.61}Ce_{0.39}F_{2.39}$, which was completely disordered and the structure of which we had investigated earlier (*5*). Laue photographs of the type Fig. 4b give partially ordered solid solutions, powder diffraction

TABLE II

CRYSTALLOGRAPHIC CHARACTERISTICS OF ORDERED PHASES WITH IDEALIZED COMPOSITION $Ca_8R_5F_{31}$ SATURATED BY RF_3 AT 1008°C

R	Parameter of the cubic pseudocell $a_{ord} = 13a_{dis} \pm 0.04$ Å	Parameter of the fluorite subcell $a_{dis} \pm 0.003$ Å	Molar volume V_{mol}, Å^3	X-ray density g/cm^3
Ho	72.05	5.542	42.55	5.29
Er	71.93	5.533	42.35	5.35
Tm	71.77	5.521	42.07	5.41
Yb	71.64	5.511	41.84	5.51
Lu	71.53	5.502	41.64	5.57
Y[a]	71.96	5.535	42.39	4.09

[a] At 915°C isotherm.

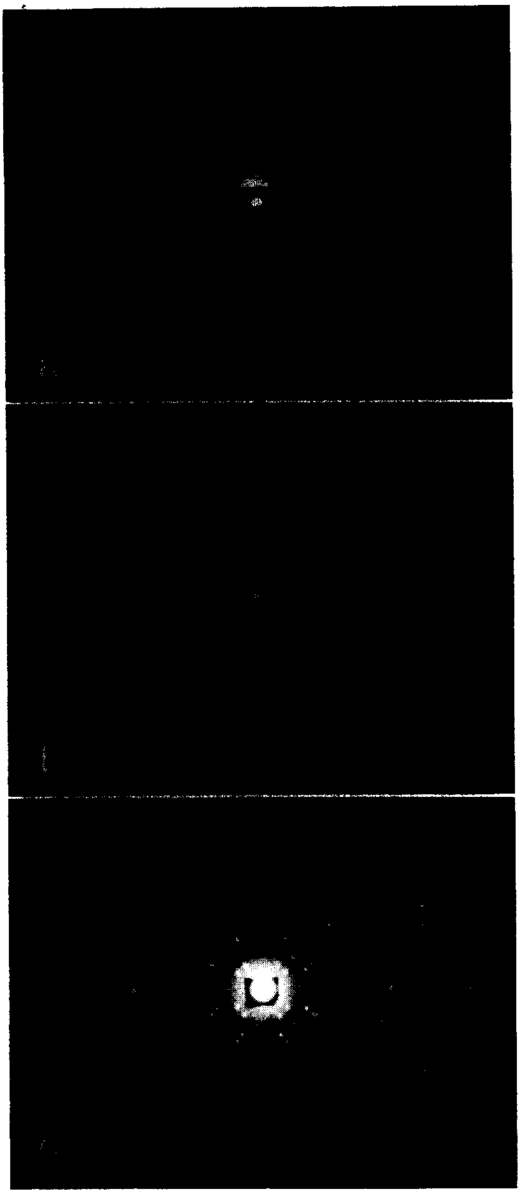

FIG. 4. Laue photographs: (a) disordered solid solution of $Ca_{0.61}Ce_{0.39}F_{2.39}$, partially ordered (b), and fully ordered (c) solid solutions $Ca_{1-x}Tm_xF_{2+x}$ ($x = 0.39 - 0.40$), Mo$K\alpha$, β.

diagrams of which have the form shown in Fig. 1b with weak superlattice reflections. X-ray rotation photographs show that the parameter of the elementary pseudocell of partially ordered phases is the same as that in fully ordered ($a_{\mathrm{ord}} = 13a_{\mathrm{dis}}$); however, in the former case, the inserted layer lines are considerably weaker. Figure 4b shows a Laue photograph of a completely ordered phase in the CaF_2–TmF_3 system (overall content 40 mole% TmF_3). This Laue photograph corresponds to a diffraction pattern of the type Fig. 1a. It is evident that the transition from partial to full ordering is expressed in increase of intensity for the supplementary reflections. Comparison of the powder diffraction patterns (Fig. 1) with the Laue photographs (Fig. 4) of the solid solutions indicates that the latter permit the ordering processes to appear at earlier stages. The interrelation of disordered solid solutions with ordered phases and their placing on the state diagrams of the CaF_2–RF_3 systems is under study.

As was indicated in (*5*), substitution of Ca^{2+} for R^{3+} in the fluorite structure is accompanied by insertion of "extra" F atoms, upon which there arise shortened $F_{\mathrm{I}}^{1-} - F_{\mathrm{II}}^{1-}$ distances in the structure. Proportional to decrease in the ionic radius of R^{3+}, the parameters of the unit cells of the solid solutions (for equal concentrations) change in the same direction and, consequently, the density of fluorine ion packing increases.

Structural investigations show that, when the ionic radius of R^{3+} decreases, local $F_{\mathrm{I}}^{1-} - F_{\mathrm{II}}^{1-}$ distances also decrease: for $Ca_{0.61}Ce_{0.39}F_{2.39}$ (*5*), they are equal to 2.31 Å, whereas for $Ca_{0.9}Y_{0.1}F_{2.1}$ (*6*), they equal 2.24 Å. At the same time, the $R^{3+} - F^{-1}$ distances exceed the sum of the ionic radii more and more during the transition from "light" to "heavy" lanthanides. Apparently, the formation of ordered phases which is expressly characteristic of systems with trifluorides of the "heavy" lanthanides is also explained by the need for compensating inequality in the interatomic spacing.

As follows from what has been said above, ordering should be manifest as much in correct spatial distribution of cations as in regular mutual orientation of the complex anion polyhedra of Ca^{2+} and R^{3+}.

The deformation of structure of the solid solutions of $(Y, Ln)F_3$ in CaF_2 described in this article is different from all other distortions of the fluorite structure known in the fluoride systems MF_2–RF_3 at the present time.

References

1. L. R. BATSANOVA, *Usp. Khim.* **40**, 945 (1971).

2. V. M. GOLDSCHMIDT AND L. THOMASSEN, *Vid. Selsk. Skr. M-N. Klasse* N2, 40 (1923).

3. A. D. FRANKLIN AND R. SPAL, *Amer. Ceram. Soc. Bull.* **54**, 320 (1972).

4. N. V. Belov, *Mineral. Sb. Lvovskovo Geol. Ob-va* **10**, 17 (1956).
5. V. B. Alexandrov and L. S. Garashina, *Dokl. Akad. Nauk SSSR* **189**, 307 (1969).
6. A. K. Cheetham, B. E. F. Fender, D. Steele, R. I. Taylor, and B. T. M. Willis, *Solid State Commun.* **8**, 171 (1970).
7. A. A. Kaminskii and V. V. Osiko, *Izv. Akad. Nauk SSSR Neorg. Mater.* **1**, 2049 (1965); *Izv. Akad Nauk SSSR Neorg. Mater.* **3**, 417 (1967); *Izv. Akad. Nauk SSSR Neorg. Mater.* **6**, 629 (1970).
8. E. G. Ippolitov, L. S. Garashina, and B. M. Zhigarnovskii, *Dokl. Akad. Nauk. SSSR* **173**, 101 (1967).
9. E. Catalano, R. G. Bedford, and H. H. Wickham, *J. Phys. Chem. Solids* **30**, 1613 (1969).
10. J. J. Stezowski and H. A. Eick, *Inorg. Chem.* **9**, 1102 (1970).
11. J. Ravez and D. Dumora, *Compt. Rend.* **269C**, 235 (1969).
12. J. Ravez and M. Duale, *Compt. Rend.* **270C**, 56 (1970).
13. J. Ravez and M. Vassiliadis, *Compt. Rend.* **270C**, 219 (1970).
14. J. Grannec and J. Ravez, *Bull. Soc. Chim. Fr.* **N5**, 1753 (1970).
15. J. Ravez, M. Darriet, R. Von der Muhl, and P. Hagenmuller, *J. Solid State Chem.* **3**, 234 (1971).
16. J. Ravez, J. Grannec, and J. Portier, *Rev. Chim. Miner.* **8**, 131 (1971).
17. J. Chassaing and A. Erb, *Compt. Rend.* **270C**, 949 (1970).
18. B. P. Sobolev, L. S. Garashina, and V. B. Aleksandrov, *Abstr. I.C.C.G.* **3**, 168, Marseilles, France, 5–9 July 1971.
19. K. B. Seyranyan, R. O. Sharkatunyan, L. S. Garashina, and B. P. Sobolev, "IV. Vsesoyuznoe Sovesh. po Rostu Kristallov," Trudi Tchast I, 127, IZd-bo AN Arm. SSR, Erevan, 1972.
20. N. G. Gogadze, E. G. Ippolitov, and B. M. Zhigarnovskii, *Zh. Neorg. Khim.* **17**, 2588 (1972).
21. R. D. Allen, *Amer. Miner.* **37**, 910 (1952).
22. A. Guinier, "Neodnorodnye Metallitcheskye Tverdye Rastvori," I. L., Moscow, 1962.